

The role of Tet3 DNA dioxygenase in epigenetic reprogramming by oocytes

Tian-Peng Gu^{1*}, Fan Guo^{1*}, Hui Yang^{2*}, Hai-Ping Wu^{1†}, Gui-Fang Xu¹, Wei Liu¹, Zhi-Guo Xie¹, Linyu Shi², Xinyi He³, Seung-gi Jin⁴, Khursheed Iqbal⁵, Yujiang Geno Shi⁶, Zixin Deng³, Piroska E. Szabó⁵, Gerd P. Pfeifer⁴, Jinsong Li² & Guo-Liang Xu¹

Sperm and eggs carry distinctive epigenetic modifications that are adjusted by reprogramming after fertilization¹. The paternal genome in a zygote undergoes active DNA demethylation before the first mitosis^{2,3}. The biological significance and mechanisms of this paternal epigenome remodelling have remained unclear⁴. Here we report that, within mouse zygotes, oxidation of 5-methylcytosine (5mC) occurs on the paternal genome, changing 5mC into 5-hydroxymethylcytosine (5hmC). Furthermore, we demonstrate that the dioxygenase Tet3 (ref. 5) is enriched specifically in the male pronucleus. In Tet3-deficient zygotes from conditional knockout mice, paternal-genome conversion of 5mC into 5hmC fails to occur and the level of 5mC remains constant. Deficiency of Tet3 also impedes the demethylation process of the paternal *Oct4* and *Nanog* genes and delays the subsequent activation of a paternally derived *Oct4* transgene in early embryos. Female mice depleted of Tet3 in the germ line show severely reduced fecundity and their heterozygous mutant offspring lacking maternal Tet3 suffer an increased incidence of developmental failure. Oocytes lacking Tet3 also seem to have a reduced ability to reprogram the injected nuclei from somatic cells. Therefore, Tet3-mediated DNA hydroxylation is involved in epigenetic reprogramming of the zygotic paternal DNA following natural fertilization and may also contribute to somatic cell nuclear reprogramming during animal cloning.

To investigate whether loss of DNA methylation in the male pronucleus coincides with oxidation of 5mC to 5hmC, a recently reported type of modification of mammalian DNA^{5,6}, we performed immunostaining of mouse zygotes using an antibody specifically recognizing 5hmC (Supplementary Fig. 1). We found that the 5hmC signal increased markedly in the paternal pronucleus around the pronuclear stage PN3 when the paternal pronucleus became larger than the maternal pronucleus (Fig. 1a, b). By contrast, the 5mC signal became markedly weaker in the male pronucleus from the PN3 stage whereas there was no clear change in the female pronucleus (Supplementary Fig. 2), as reported previously². The inverse correlation between the 5hmC and 5mC signals in the two parental genomes seemed to persist beyond the zygotic stage (Supplementary Fig. 3). Therefore, 5mC oxidation in the male pronucleus coincides with the loss of methylation in the early mouse embryo. A similar observation has recently been reported in two independent studies^{7,8}.

Next, we examined the expression of Tet enzymes that can catalyse the oxidation of 5mC in DNA⁹. The *Tet3* mRNA was specifically detected in oocytes and zygotes (Supplementary Fig. 4). At the zygotic stage, the Tet3 protein was concentrated in the male pronucleus, but localized to the cytoplasm at other pre-implantation stages (Fig. 1c and Supplementary Fig. 5). The unique expression pattern of Tet3 suggests its possible role in modifying the zygotic paternal genome.

To study the biological function of Tet3 in mouse, we generated a conditional knockout allele abolishing its catalytic activity (Supplementary Fig. 6a). Because homozygous mutation led to neonatal lethality, we achieved germ-line-specific deletion of Tet3 from primordial germ cells (PGCs) in [*Tet3*^{f/f}, TNAP-Cre] conditional knockout (CKO) mice.

Female CKO mice were normal in growth and morphology. Although they displayed much reduced fecundity (see below), they gave birth to heterozygous offspring when crossed with wild-type males (Supplementary Fig. 6b). The deletion of Tet3 in oocytes and zygotes was confirmed by immunostaining and PCR with reverse transcription assays (Fig. 2a and Supplementary Fig. 6c). Strikingly, no 5hmC signal could be detected and the 5mC signal intensity did not decline in the late male pronuclei of zygotes collected from the CKO females mated with wild-type males (Fig. 2b and Supplementary Fig. 7). In contrast, deletion of *Tet3* from the male germ cells did not seem to affect the change in 5hmC and 5mC. Therefore, the loss of 5mC in the paternal genome in developing zygotes is caused by its conversion to 5hmC and the maternal Tet3 is required for this conversion.

We then assessed the role of Tet3 in demethylation of specific sequences in the male pronucleus. *Line1* transposons are known to be actively demethylated in zygotes^{10,11}. Comparison of the methylation level of male pronuclear DNA from Tet3-deficient zygotes at the PN3–4 stages with that of wild-type zygotes showed that the process of active DNA demethylation was impeded by Tet3 deletion (Fig. 2c, upper panel). This finding also indicates that 5hmC serves as an intermediate between 5mC and unmethylated C, although bisulphite analysis cannot distinguish 5hmC from 5mC^{12,13}. To confirm this, we assayed for 5mC and 5hmC on *Line1* elements in the paternal DNA by MeDIP and hMeDIP (methylated and hydroxymethylated DNA immunoprecipitation). 5hmC was indeed present at *Line1* sequences in wild-type zygotic male pronuclei at a significantly higher level compared to sperm, whereas the 5mC level was markedly lower than that of sperm (Supplementary Fig. 8). In the analysis of male pronuclear DNA from zygotes lacking Tet3, enrichment of 5hmC-containing *Line1* elements was significantly decreased whereas enrichment of 5mC-containing elements was comparable with sperm. These results strengthen the conclusion that 5mC oxidation does occur at *Line1* sequences in male pronuclei.

Embryonic stem cell marker genes, such as *Oct4* and *Nanog*, are methylated during male germ cell development and their demethylation occurs in the early embryo^{14–16}. In normal zygotes, the *Oct4* gene of male pronuclei had undergone substantial demethylation by the PN3–4 pronuclear stages, but this process was markedly hampered in Tet3-null zygotes (Fig. 2c and Supplementary Fig. 9). Moreover, Tet3 deletion almost completely blocked demethylation at two other

¹Group of DNA Metabolism, The State Key Laboratory of Molecular Biology, Institute of Biochemistry and Cell Biology, Shanghai Institutes for Biological Sciences, Chinese Academy of Sciences, Shanghai 200031, China. ²The State Key Laboratory of Cell Biology, Institute of Biochemistry and Cell Biology, Shanghai Institutes for Biological Sciences, Chinese Academy of Sciences, Shanghai 200031, China. ³The State Key Laboratory of Microbial Metabolism, School of Life Science and Biotechnology, Shanghai Jiaotong University, Shanghai 200030, China. ⁴Department of Cancer Biology, Beckman Research Institute of the City of Hope, Duarte, California 91010, USA. ⁵Department of Molecular and Cellular Biology, Beckman Research Institute of the City of Hope, Duarte, California 91010, USA. ⁶Division of Endocrinology, Diabetes, and Hypertension, Department of Medicine and BCMP, Brigham and Women's Hospital and Harvard Medical School, Boston, Massachusetts 02115, USA. [†]Present address: Novartis Institutes for BioMedical Research Co., Shanghai 201203, China.

*These authors contributed equally to this work.

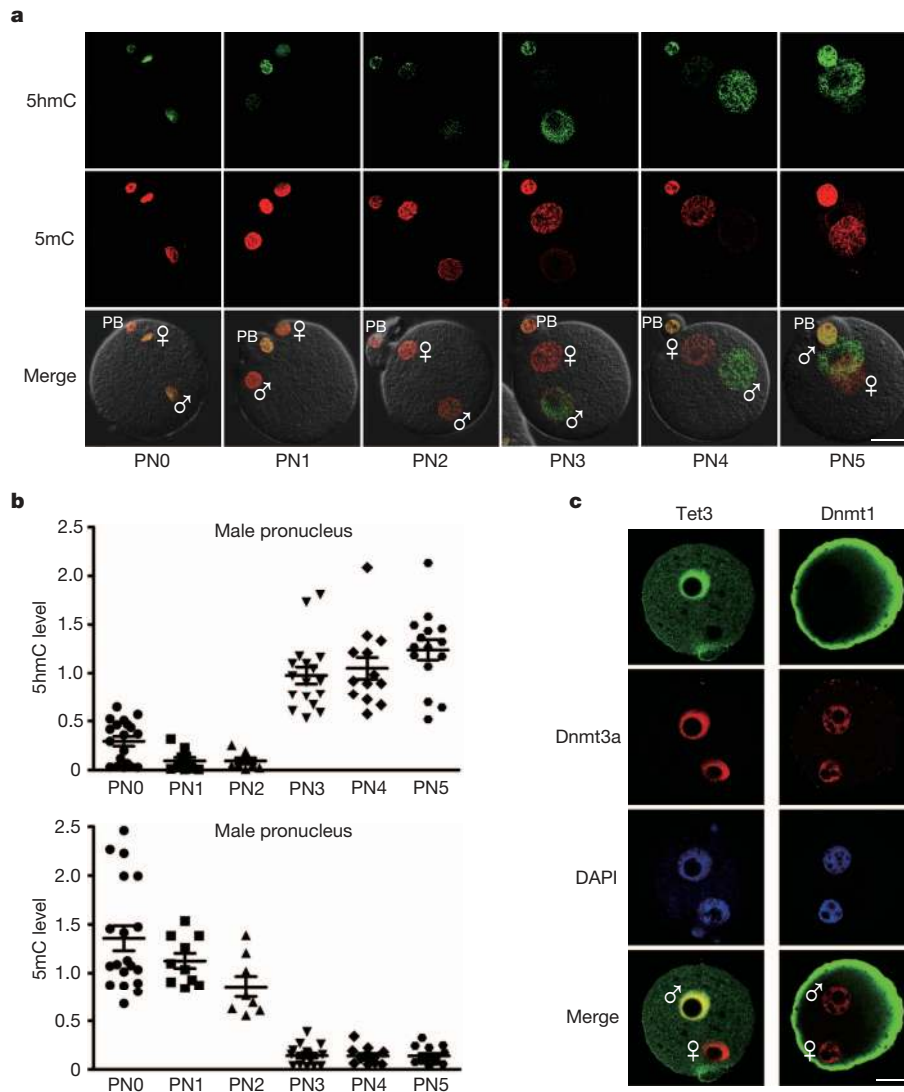


Figure 1 | Specific oxidation of methylcytosine and Tet3 distribution in the zygotic male pronucleus. **a**, Immunofluorescent images of 5hmC (green) and 5mC (red) staining, and overlaid phase contrast images. The pronuclear (PN) stages are indicated. Male and female symbols indicate male and female pronucleus, respectively. PB, polar body. Scale bar, 25 μ m. **b**, Quantification of the relative levels of 5hmC and 5mC in male pronuclei in zygotes. Each data point is based on the level of the 5hmC or 5mC signal relative to the DAPI

staining intensity of the same pronucleus. Error bars indicate s.e.m. Number of zygotes analysed for each stage: PN0, 19; PN1, 10; PN2, 8; PN3, 17; PN4, 17; PN5, 15. **c**, Preferential staining of Tet3 protein in the male pronucleus. DNA was stained with DAPI. Control staining shows Dnmt1 in the cortical cytoplasm and Dnmt3a (red) in both pronuclei. The nucleolus had no staining signal.

paternally methylated genes, *Nanog* and *Lemdl* (ref. 17), which retained hypermethylation similar to that observed in sperm (Supplementary Fig. 9). To assess the significance of paternal demethylation on gene expression, Tet3-null oocytes from the CKO females were fertilized by intracytoplasmic injection (ICSI) of wild-type sperm carrying the enhanced green fluorescent protein (EGFP) reporter gene under the control of the *Oct4* promoter, and expression of EGFP was monitored in cultured embryos. Compared with wild-type embryos, the mutant embryos derived from oocytes lacking Tet3 showed significantly weaker EGFP expression at the 8-cell and morula stages (Fig. 2d and Supplementary Fig. 10). Based on these global and sequence-specific analyses of 5mC and 5hmC, along with the reporter gene assay, we conclude that Tet3-mediated 5mC oxidation contributes to the demethylation in the zygotic paternal genome and gene activation in the early embryo.

We next investigated whether removing Tet3 from oocytes might compromise embryonic development. We first confirmed that early deletion of Tet3 from the PGC stage did not affect epigenetic reprogramming in the embryonic germ cells, oocyte development,

maturation and fertilization (Supplementary Figs 11–13 and Supplementary Table 1). Male germ cell development and sperm DNA methylation were not affected either (Supplementary Fig. 14). However, fecundity of the female CKO mice was significantly lower in terms of the frequency of successful pregnancy per mating and the litter size (Fig. 3a and Supplementary Table 2).

Deletion of maternal Tet3 did not seem to affect the pre-implantation development as heterozygous zygotes collected from CKO females mated with wild-type males developed to blastocysts *in vitro* normally (Supplementary Table 3). We then examined the effect of maternal Tet3 deletion on prenatal development by transplantation of 2-cell embryos into oviducts of pseudo-pregnant females. Whereas the transferred embryos lacking maternal Tet3 implanted normally, they showed a much reduced rate of full-term development (Supplementary Table 4). Dissection of transferred [*Tet3* *Mat*⁻/*Pat*⁺] mutant embryos in the pregnant wild-type foster mothers revealed a high frequency of degeneration and the appearance of morphological abnormalities, starting from midgestation (Fig. 3b and Supplementary Table 4). Moreover, deletion of Tet3 later from growing oocytes

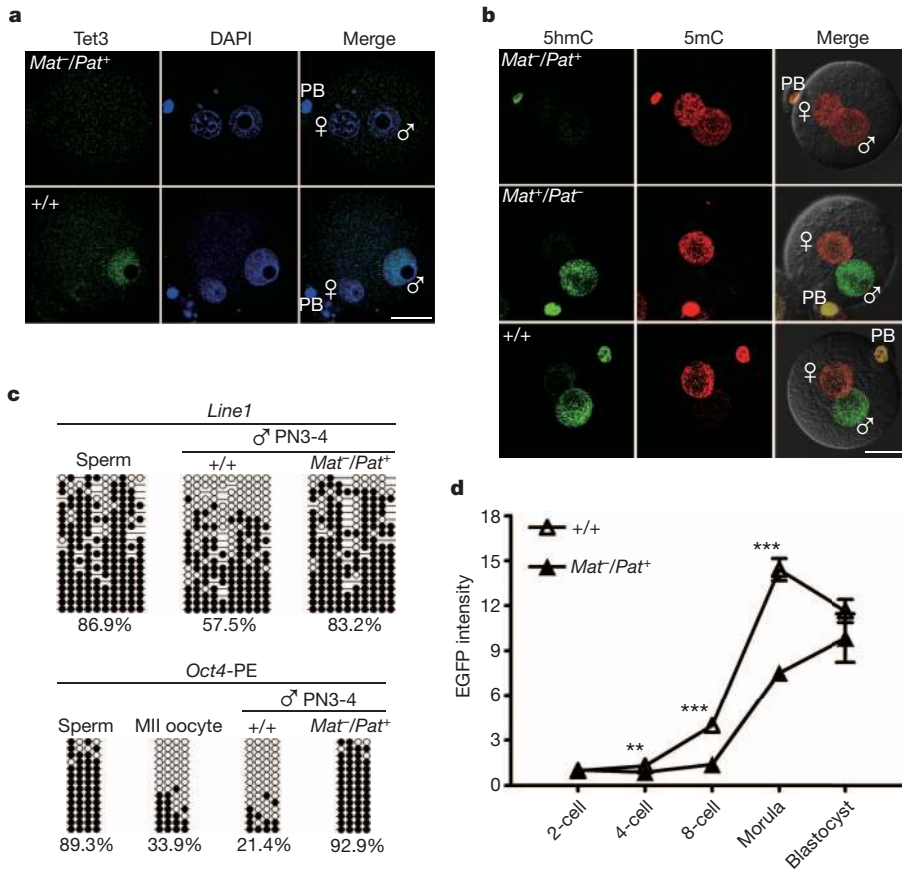


Figure 2 | The role of Tet3 in 5mC oxidation, demethylation of paternal DNA, and activation of the paternal *Oct4* allele. **a**, Loss of the Tet3 protein in heterozygous zygotes (*Mat⁻/Pat⁺*) obtained from CKO females mated with wild-type males. PN3 zygotes were stained with an anti-Tet3 antibody raised against the deleted region. Scale bar, 25 μ m. **b**, 5hmC (green) and 5mC (red) immunostaining in wild-type (*+/+*) and maternally (*Mat⁻/Pat⁺*) or paternally (*Mat⁺/Pat⁻*) Tet3-deficient zygotes at the PN5 stage. **c**, Methylation analysis of *Line1* and *Oct4* (PE, the proximal enhancer region) in male pronuclei isolated from wild-type (*+/+*) and Tet3-deficient (*Mat⁻/Pat⁺*) zygotes. Open and filled circles represent unmethylated and methylated CpG sites, respectively. Percentage of methylated CpGs is indicated. **d**, Paternal *Oct4* activation in wild-type embryos (*+/+*) and embryos lacking maternal Tet3 (*Mat⁻/Pat⁺*). Embryos were derived from ICSI using sperm carrying the *Oct4-EGFP* transgene and the EGFP signal was quantified, relative to the level in a 2-cell blastomere. Number of embryos analysed at each stage, *+/+*: 2-cell, 13; 4-cell, 9; 8-cell, 9; morula, 12; blastocyst, 7. *Mat⁻/Pat⁺*: 2-cell, 11; 4-cell, 9; 8-cell, 8; morula, 8; blastocyst, 5. Error bars indicate s.e.m. ** $P < 0.01$ and *** $P < 0.001$.

using *Zp3-Cre* also led to failure in zygotic 5hmC generation, retention of paternal 5mC, impaired demethylation at *Line1* and *Oct4*, and compromised embryonic development (Supplementary Fig. 15). Therefore, lacking maternal Tet3 blocks paternal genome reprogramming and causes markedly increased developmental failure of the embryo.

Somatic cell nuclei injected into eggs undergo profound epigenetic reprogramming, including DNA demethylation. The cytoplasm of germinal vesicle (GV) oocytes¹⁸, metaphase II (MII) oocytes¹⁹, zygotes²⁰ and 2-cell embryos²¹ has been shown to possess reprogramming activity. The existence of the Tet3 protein across these stages indicated that Tet3 might be one of the cytoplasmic factors contributing to the reprogramming activity. We tested therefore whether Tet3-mediated hydroxylation is part of the reprogramming process in somatic cell nuclear transfer (SCNT). Remarkably, following activation of nuclear transfer (NT) oocytes reconstructed after injection of somatic nucleus into oocyte with or without enucleation (intact oocyte), the Tet3 protein originating from the oocyte cytoplasm became concentrated in the pseudo-pronucleus (PPN) formed from the transferred somatic nucleus, but not in the female pronucleus derived from the spindle-chromosome-complex that existed in oocytes (Fig. 4a). Significantly, the PPN formed in the NT embryos from wild-type intact or enucleated oocytes underwent 5mC oxidation whereas this modification did not occur in embryos derived from Tet3-null oocytes (Fig. 4b). Whereas substantial demethylation was detected at the *Oct4* promoter in the PPN of Tet3-proficient NT embryos, the somatic hypermethylation persisted when the oocyte Tet3 was deleted (Fig. 4c). To investigate the role of Tet3-mediated DNA oxidation in the activation of pluripotency genes, we used donor somatic cells carrying the *Oct4-EGFP* transgene. Compared with embryos from wild-type oocytes, the EGFP signal was significantly lower in embryos derived from the Tet3-null oocytes at the

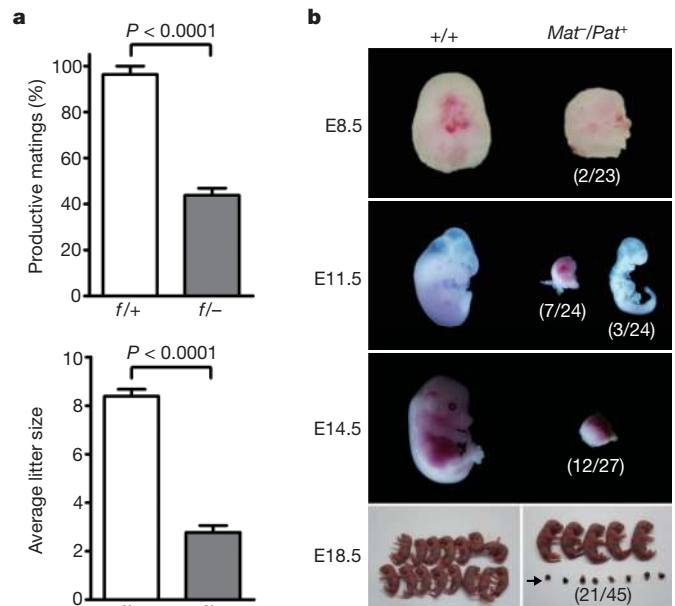


Figure 3 | Maternal Tet3 deficiency compromises embryonic development. **a**, Reduced efficiency of productive mating and litter size in females (*f/-*) with germline Tet3 deficiency. Error bars indicate s.e.m. [*Tet3^{f/+}*, TNAP-Cre] mice, $n = 9$; [*Tet3^{f/-}*, TNAP-Cre] mice, $n = 7$. **b**, Developmental failure among embryos lacking maternal Tet3. Pregnant foster females receiving wild-type (*+/+*) and mutant (*Mat⁻/Pat⁺*) 2-cell embryos transferred were dissected at different stages of gestation. Numbers in brackets indicate proportion of embryonic day 8.5 (E8.5) deciduas and E11.5–18.5 embryos showing a smaller size and morphological abnormalities. The arrow indicates degenerated conceptuses obtained. Detailed data are presented in Supplementary Table 4.

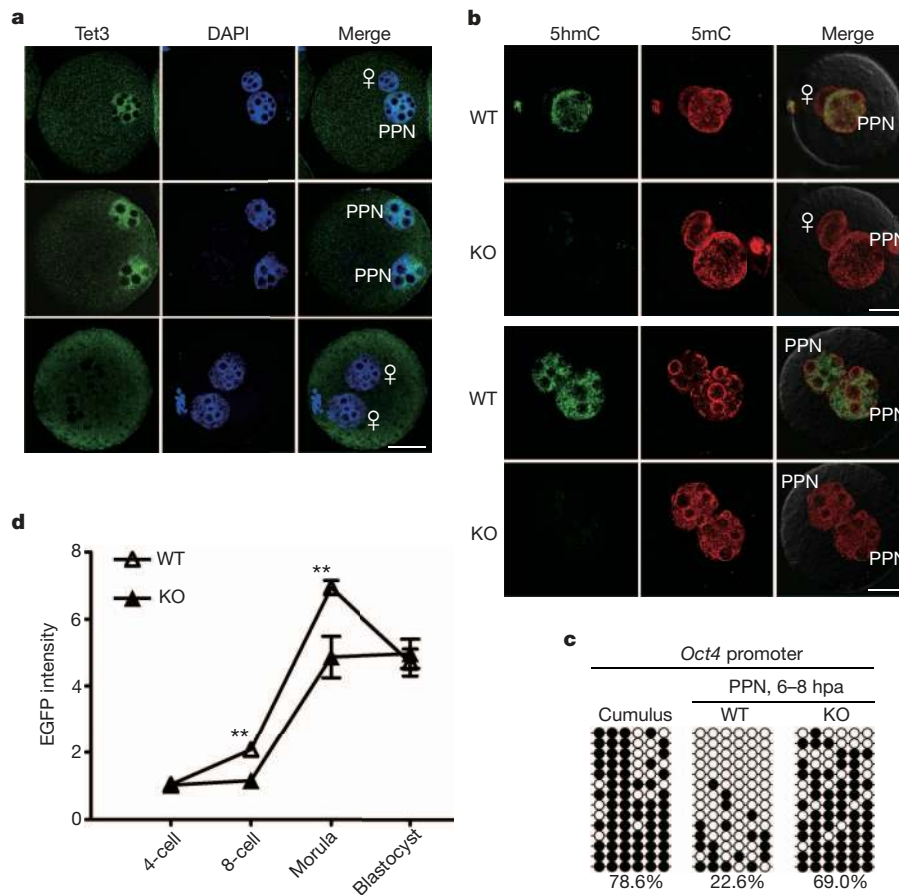


Figure 4 | Tet3 contributes to reprogram the somatic nucleus transferred into oocytes. **a**, Tet3 enrichment in the pseudo-pronucleus (PPN) formed in embryos reconstructed by transplantation of cumulus somatic nuclei into an intact (top row) or enucleated oocyte (middle row). The enrichment did not occur in the female pronucleus in intact oocytes (top row) and in the two pronuclei of parthenogenetic embryos (bottom row). Scale bar, 25 μ m. **b**, Impaired 5mC oxidation in PPN of 1-cell NT embryos derived from injection of cumulus nuclei into intact or enucleated oocytes lacking Tet3. Embryos around 10 h post activation (hpa) were stained with anti-5hmC (green) and

anti-5mC (red) antibodies. **c**, Impaired *Oct4* demethylation in NT embryos derived from Tet3-null oocytes. More than 20 NT embryos derived from enucleated wild-type (WT) or Tet3-null (KO) oocytes were collected 6–8 hpa for DNA methylation analysis. **d**, Weakened activation of the somatic *Oct4-EGFP* reporter in cultured NT embryos from Tet3-null oocytes. The EGFP intensities were relative to the level in a 4-cell blastomere. Error bars indicate s.e.m. Number of embryos analysed for each stage, WT: 4-cell, 11; 8-cell, 13; morula, 9; blastocyst, 7. KO: 4-cell, 8; 8-cell, 7; morula, 6; blastocyst, 7. $**P < 0.01$.

8-cell and morula stages (Fig. 4d and Supplementary Fig. 16a). Consistently, the *Oct4* mRNA level was relatively low in 8-cell embryos from Tet3-null oocytes (Supplementary Fig. 16b). Therefore, deficiency in oocyte Tet3 could cause weakened or delayed activation of the somatic *Oct4* in NT embryos.

We have obtained substantial evidence that oxidation of 5mC in the paternal genome in fertilized eggs by Tet3 initiates DNA demethylation and facilitates the activation of the paternal copy of early embryonic genes, thus contributing to the establishment of biparental totipotency in the early embryo by counteracting the silencing function of 5mC. Blocking oxidation of 5mC by Tet3 deletion affects paternal gene activation, leading to reduced developmental fitness and fetal survival. It remains to be determined whether the developmental failures could be caused by haploinsufficiency²² for the genes affected in the early embryo.

The involvement of Tet3 in somatic *Oct4* activation indicates that Tet-mediated 5mC oxidation contributes to epigenetic reprogramming of the donor nuclear DNA in SCNT. Reprogramming in SCNT might thus share a common mechanism with paternal genome remodelling in fertilized eggs. Further investigations are needed to reveal the signals regulating Tet3 and the events subsequent to 5hmC formation in both fertilized and cloned embryos.

METHODS SUMMARY

Preparation of anti-5hmC antibody. To prepare anti-5hmC antibody, 5-hydroxymethylcytidine 5'-monophosphate (5hmCMP) hapten was synthesized from cytidine 5'-monophosphate (CMP) using MilA hydroxymethylase²³. The ribonucleoside was then conjugated to bovine serum albumin (BSA) as previously described²⁴ and used to immunize rabbits. The antibody was affinity-purified from antiserum with 5hmCMP-BSA conjugate coupled to agarose beads.

Immunostaining for 5hmC in fertilized oocytes. Immunofluorescence detection of 5hmC in zygotes followed the procedure for 5mC¹¹. Fluorescent images were acquired at 2- μ m Z-axis intervals using a confocal microscope (LEICA TCS SP5 II) and their signal intensity was determined.

Gene targeting. A *Tet3* targeting vector was electroporated into 129Sv ES cells for homologous recombination. The floxed region contains exons 8-9, which includes the coding region for the conserved Fe²⁺-binding motif of dioxygenases. To inactivate *Tet3* in the germ line, we crossed the mice carrying a floxed allele with TNAP-Cre knock-in mice on a 129 genetic background²⁵. The conditional knock-out mice were on C57BL/6J-129Sv genetic background.

Zygote collection and staging. Female mice 4- to 8-week-old were injected with pregnant mare's serum gonadotropin and human chorionic gonadotropin were mated with wild-type males. Zygotes were harvested and the PN stages of individual zygotes were classified according to ref. 11, by taking into account the pronuclear morphology and the presence of 5mC signal.

Observation of *Oct4-EGFP* activation. To examine the role of Tet3 in paternal gene activation, MII oocytes collected from wild-type and Tet3 CKO females were

fertilized by ICSI with sperm from transgenic mice (tg/tg) carrying the *Oct4-EGFP* transgene²⁶ and the resulting embryos were cultured to observe EGFP expression. To examine the role of Tet3 in somatic gene activation in SCNT, we monitored the *Oct4-EGFP* transgene expression from the donor cell DNA in NT embryos, which were derived after injection of a cumulus nucleus into a wild-type or a Tet3-null oocyte without enucleation.

Full Methods and any associated references are available in the online version of the paper at www.nature.com/nature.

Received 21 January; accepted 16 August 2011.

Published online 4 September 2011.

- Surani, M. A., Hayashi, K. & Hajkova, P. Genetic and epigenetic regulators of pluripotency. *Cell* **128**, 747–762 (2007).
- Mayer, W., Niveleau, A., Walter, J., Fundele, R. & Haaf, T. Demethylation of the zygotic paternal genome. *Nature* **403**, 501–502 (2000).
- Oswald, J. *et al.* Active demethylation of the paternal genome in the mouse zygote. *Curr. Biol.* **10**, 475–478 (2000).
- Ooi, S. K. & Bestor, T. H. The colorful history of active DNA demethylation. *Cell* **133**, 1145–1148 (2008).
- Tahiliani, M. *et al.* Conversion of 5-methylcytosine to 5-hydroxymethylcytosine in mammalian DNA by MLL partner TET1. *Science* **324**, 930–935 (2009).
- Kriaucionis, S. & Heintz, N. The nuclear DNA base 5-hydroxymethylcytosine is present in Purkinje neurons and the brain. *Science* **324**, 929–930 (2009).
- Iqbal, K., Jin, S. G., Pfeifer, G. P. & Szabo, P. E. Reprogramming of the paternal genome upon fertilization involves genome-wide oxidation of 5-methylcytosine. *Proc. Natl Acad. Sci. USA* **108**, 3642–3647 (2011).
- Wossidlo, M. *et al.* 5-Hydroxymethylcytosine in the mammalian zygote is linked with epigenetic reprogramming. *Nature Commun.* **2**, 241 (2011).
- Wu, S. C. & Zhang, Y. Active DNA demethylation: many roads lead to Rome. *Nature Rev. Mol. Cell Biol.* **11**, 607–620 (2010).
- Jamil, A. Z., Iqbal, K., Fawad Ur, R. & Mirza, K. A. Effect of phacoemulsification on intraocular pressure. *J. Coll. Physicians Surg. Pak.* **21**, 347–350 (2011).
- Wossidlo, M. *et al.* Dynamic link of DNA demethylation, DNA strand breaks and repair in mouse zygotes. *EMBO J.* **29**, 1877–1888 (2010).
- Jin, S. G., Kadam, S. & Pfeifer, G. P. Examination of the specificity of DNA methylation profiling techniques towards 5-methylcytosine and 5-hydroxymethylcytosine. *Nucleic Acids Res.* **38**, e125 (2010).
- Huang, Y. *et al.* The behaviour of 5-hydroxymethylcytosine in bisulfite sequencing. *PLoS ONE* **5**, e8888 (2010).
- Hattori, N. *et al.* Epigenetic control of mouse *Oct-4* gene expression in embryonic stem cells and trophoblast stem cells. *J. Biol. Chem.* **279**, 17063–17069 (2004).
- Imamura, M. *et al.* Transcriptional repression and DNA hypermethylation of a small set of ES cell marker genes in male germline stem cells. *BMC Dev. Biol.* **6**, 34 (2006).
- Farthing, C. R. *et al.* Global mapping of DNA methylation in mouse promoters reveals epigenetic reprogramming of pluripotency genes. *PLoS Genet.* **4**, e1000116 (2008).
- Iqbal, K. *et al.* Subcutaneous panniculitis-like T-cell lymphoma in association with sarcoidosis. *Clin. Exp. Dermatol.* **36**, 677–679 (2011).
- Bui, H. T. *et al.* The cytoplasm of mouse germinal vesicle stage oocytes can enhance somatic cell nuclear reprogramming. *Development* **135**, 3935–3945 (2008).
- Yang, H. *et al.* High-efficiency somatic reprogramming induced by intact MII oocytes. *Cell Res.* **20**, 1034–1042 (2010).
- Eggle, D., Rosains, J., Birkhoff, G. & Eggen, K. Developmental reprogramming after chromosome transfer into mitotic mouse zygotes. *Nature* **447**, 679–685 (2007).
- Eggle, D., Sandler, V. M., Shinohara, M. L., Cantor, H. & Eggen, K. Reprogramming after chromosome transfer into mouse blastomeres. *Curr. Biol.* **19**, 1403–1409 (2009).
- Seidman, J. G. & Seidman, C. Transcription factor haploinsufficiency: when half a loaf is not enough. *J. Clin. Invest.* **109**, 451–455 (2002).
- Li, L. *et al.* The mildiomycin biosynthesis: initial steps for sequential generation of 5-hydroxymethylcytidine 5'-monophosphate and 5-hydroxymethylcytosine in *Streptovorticillium rimofaciens* ZJU5119. *ChemBioChem* **9**, 1286–1294 (2008).
- Erlanger, B. F. & Beiser, S. M. Antibodies specific for ribonucleosides and ribonucleotides and their reaction with DNA. *Proc. Natl Acad. Sci. USA* **52**, 68–74 (1964).
- de Vries, W. N. *et al.* Expression of Cre recombinase in mouse oocytes: a means to study maternal effect genes. *Genesis* **26**, 110–112 (2000).
- Ohbo, K. *et al.* Identification and characterization of stem cells in prepubertal spermatogenesis in mice. *Dev. Biol.* **258**, 209–225 (2003).

Supplementary Information is linked to the online version of the paper at www.nature.com/nature.

Acknowledgements We thank C. Walsh and M. Rots for critical reading of the manuscript, J. Walter for discussions, H. Qi for providing cDNA of mouse oocytes, R. Zhang & Q. Cui for *Tet3* cDNA, L. Li for help with 5hmCMP synthesis, Shanghai Research Center for Model Organisms for blastocyst injection, and J. Gao for mouse work. This study was supported by grants from the Ministry of Science and Technology China (2007CB947503 to G.-L.X., 2007CB947101 to J.L., and 2009CB941101 to G.-L.X. and J.L.), National Science Foundation of China (30730059 to G.-L.X. and 30871430 to J.L.), the Chinese Academy of Sciences (XDA01010301 to G.-L.X.; XDA01010403 and KSCX2-YW-R-110 to J.L.) and the NIH (GM078458 to Y.G.S.).

Author Contributions G.-L.X. and J.L. conceived the projects. Y.G.S., H.-P.W. and G.-L.X. contributed to the knockout design. F.G., T.-P.G., H.-P.W., G.-F.X., and W.L. performed the experiments on early embryos. X.H. and Z.D. contributed to the synthesis of the 5hmC hapten. H.Y. and L.S. performed the nuclear transfer and embryo transfer experiments. S.-g.J., K.I., P.E.S., G.P.P. and Z.-G.X. characterized Tet3 expression in PGCs and ovaries. G.-L.X. wrote and G.P.P. revised the manuscript.

Author Information Reprints and permissions information is available at www.nature.com/reprints. The authors declare no competing financial interests. Readers are welcome to comment on the online version of this article at www.nature.com/nature. Correspondence and requests for materials should be addressed to J.L. (jsli@sibs.ac.cn) or G.-L.X. (glxu@sibs.ac.cn).

METHODS

Preparation of anti-5hmC and anti-Tet3 antibodies. To prepare 5hmC antibody, 5-hydroxymethylcytidine 5'-monophosphate (5hmCMP) hapten was synthesized from cytidine 5'-monophosphate (CMP) in a reaction containing formaldehyde and tetrahydrofolate catalysed by recombinant MilA hydroxymethylase²³. The ribonucleoside hapten was then conjugated to BSA as previously described²⁴ for immunization of rabbits (Supplementary Fig. 1). Mass spectral analysis confirmed that the 5hmCMP base moiety was unaltered under the conjugation condition. The antibody was affinity-purified from antiserum with the 5hmCMP-BSA conjugate coupled to agarose beads. To ensure specificity, cross-reactivity was removed by incubation with agarose beads crosslinked with CMP-BSA conjugate.

For the detection of Tet3, two rabbit polyclonal antibodies were raised against a C-terminal region (amino acids 1159–1329, GenBank accession number NP_898961) and the targeted region (amino acids 887–962) respectively, affinity-purified and evaluated as described previously²⁷.

Immunostaining for 5hmC and Tet3 in fertilized oocytes. Immunofluorescence detection of 5hmC in zygotes derived from natural matings followed the procedure for 5mC¹¹. The signal was detected by Alexa Fluor-conjugated goat anti-rabbit or anti-mouse IgG (see Supplementary Table 4 for detailed antibody information). Fluorescent images were acquired at 2- μ m Z-axis intervals using a confocal microscope (Leica TCS SP5 II) and their signal intensity was determined using the Leica Application Suite-Advanced Fluorescence software.

The distribution of the Tet3 protein in embryonic cells was determined on embryos fixed with 4% paraformaldehyde (PFA) and permeabilized with 0.5% Triton.

Gene targeting. A targeting vector for *Tet3* was prepared using the recombinering technique²⁸ and electroporated into 129Sv ES cells for selection of targeted clones. The floxed region contains exons 8–9, which code for the region (76 amino acids from EEVLR to NGCTV, GenBank accession number NP_898961) containing the conserved Fe²⁺-binding motif of the catalytic domain. Deletion of the floxed region leads to the loss of 76 amino acids with in-frame fusion between exons 7 and 10. Neomycin-resistant embryonic stem clones were screened by PCR using a pair of primers crossing the shorter right homologous arm. Positive clones were further characterized by Southern blotting to confirm homologous recombination on the left side of the targeted genomic region (refer to Supplementary Fig. 7a). Embryonic stem cells carrying a correctly targeted allele (with *neo*) were injected into blastocysts to generate germline chimaeras. Mice with a floxed allele were obtained by breeding with C57BL/6J mice. The *neo* selection marker was removed in mice by crossing with ACTFLPe mice²⁹. To inactivate *Tet3* in germ cells from the PGC stage onwards, we generated conditional knockout mice by crossing floxed mice with TNAP-Cre knock-in mice. TNAP-Cre is expressed in primordial germ cells from embryonic day 9.5 to late gestation³⁰. To inactivate *Tet3* in female germ cells from the growing oocyte stage, we generated conditional knockout mice by crossing floxed mice with Zp3-Cre transgenic mice which express Cre exclusively in growing oocytes³¹. Mice were genotyped by PCR (primer sequences are presented in Supplementary Table 6). The conditional knockout mice were on a mixed C57BL/6J-129Sv genetic background.

Zygote collection. Wild-type BDF1 (from C57BL/6 \varnothing \times DBA2 σ) female mice 4- to 8-week-old injected with pregnant mare's serum gonadotropin and human chorionic gonadotropin were mated with BDF1 male. Zygotes were harvested at different time points after human chorionic gonadotropin injection. The PN stage of each individual zygote was classified according to ref. 11, by taking into account the pronuclear morphology and the presence of 5mC signal. We stained the DNA with DAPI (for fixed zygotes) or Hoechst 33258 (for live zygotes), and used a Nomarski differential interference contrast microscope for better observation of zygotic pronuclei, when necessary. Tet3-deficient zygotes were obtained from [*Tet3*^{fl/fl}, TNAP-Cre] female mice crossed with wild-type males.

Fertility test. [*Tet3*^{fl/fl}, TNAP-Cre] female mice at 6–8 weeks of age were housed with 8- to 12-week-old wild-type males of proven fertility. Rate of fertilization was judged by the presence of two pronuclei in zygotes collected from females after pregnant mare's serum gonadotropin and human chorionic gonadotropin treatment and mating with wild-type male mice of proven fertility. Number of completed pregnancies per plug seen (litters per plug) and number of viable pups born per litter (litter size) were calculated from the data included in Supplementary Table 2. [*Tet3*^{fl/fl}, TNAP-Cre] female mice were used as a control group for comparison. Student's *t*-test was performed to compare averages in the two different experimental groups and *P* < 0.05 was considered to be significant.

Isolation of primordial germ cells (PGCs). Female CFI (Charles River Laboratories) mice were mated with male OG2 (ref. 32) mice. This transgenic mouse line expresses the enhanced green fluorescent protein (EGFP) from the *Oct4* promoter and thus enables the selective purification of embryonic and fetal germ cells. Embryo parts enriched in PGCs and genital ridges were dissected at 9.5

and 11.5 days post coitum (dpc), respectively. At 9.5 dpc and 11.5 dpc, the sex of the embryo was determined by real-time PCR amplification of two genes in a single reaction. The *Sry* amplicon indicated the presence of Y chromosome and male sex, whereas amplification of the *Snrpn* gene served as a positive control for DNA. Gonads were dissected from male and female fetuses at 13.5, 15.5 and 17.5 dpc. Male and female gonads were distinguished by their distinct morphology at these stages. Gonads were incubated at 37 °C for 15 min in trypsin-EDTA and triturated to achieve a single cell suspension containing germ cells and somatic cells. Dulbecco's Modified Eagle's Medium (DMEM) (Invitrogen) supplemented with 20% FBS was added to inactivate trypsin. Cell suspensions were analysed and sorted on a MoFlo flow cytometer (Beckman Coulter). Data were acquired using 488 nm excitation from an Innova-306 Argon laser (Coherent) at 500 mW. EGFP emission was measured through a 530DF30 filter (Omega Optical).

Quantitative reverse transcription PCR. Poly(A⁺) mRNAs were isolated from zygotes (*n* = 200) and female PGCs (embryonic days 9.5, 11.5, 13.5, 15.5 and 17.5) by using the Dynabeads mRNA DIRECT Micro Kit (Invitrogen). Oligo (dT)25-coupled Dynabeads and mRNA complexes were immediately used for reverse transcription using SuperScript III reverse transcriptase (Invitrogen), according to the manufacturer's instructions. Real-time quantitative PCR reactions were performed at 50 °C for 2 min and 95 °C for 10 min followed by 50 cycles at 95 °C for 15 s and 60 °C for 1 min using TaqMan Gene Expression Master Mix (Applied Biosystems) on an iQ5 real-time PCR cycler (Bio-Rad). PCR was performed with TaqMan MGB primers with 6FAM-based probes (Applied Biosystems) using the following assay ID numbers: *Tet1* (Mm01169088_m1), *Tet2* (Mm01312907_m1), *Tet3* (Mm00805754_m1) and *Stella/Dppa3* (Mm01184198_g1). The cDNA levels of target genes were analysed using a comparative *C_t* method and normalized to the internal standard gene *Gapdh*.

Collection of oocytes and production of parthenogenetic embryos. For collection of GV oocytes, the ovaries were removed from the female mice 42–44 h after pregnant mare's serum gonadotropin injection. Antral follicles were punctured by 30G needles, and cumulus-enclosed GV oocytes were released into HEPES-buffered CZB medium (HCZB) containing 0.2 mM 3-isobutyl-1-methylxanthine (IBMX) to inhibit germinal vesicle breakdown. Cumulus cells were removed by pipetting. For collection of mature oocytes, oviducts were removed from the female mice 13–15 h after human chorionic gonadotropin injection. Cumulus-oocyte complexes were released into HCZB containing 0.1% bovine testicular hyaluronidase (300 USP units per mg; ICN Biomedicals Inc.). MII oocytes were activated for 6 h in activation medium (calcium-free CZB medium containing 10 mM Sr²⁺ and 5 μ g ml⁻¹ cytochalasin B) to generate parthenogenetic embryos, which were cultured in KSOM medium with amino acids and harvested at 8 h post activation.

Intracytoplasmic sperm injection (ICSI). ICSI was performed according to the method of ref. 33 except for being performed at room temperature (about 25 °C). Briefly, sperm were collected from adult mice (Oct-delta PE-GFP #18) carrying *Oct4-EGFP* transgene (tg/tg)²⁶ and the head was separated from the tail by applying pulses to the head-tail junction by means of a Piezo-driven pipette (Piezoelectric actuator; PrimeTech). Only the sperm head was injected into each oocyte. Injected oocytes were cultured in KSOM medium for 96 h to examine their development *in vitro*. Images of resulting embryos were acquired with an IX51 inverted microscope (Olympus) under the same exposure parameters and the EGFP intensity of each embryo was quantified with ImageJ software³⁴.

Embryo transfer and Caesarean section. Fertilized eggs derived from natural matings were cultured in KSOM medium until the 2-cell stage. Two-cell embryos were then transferred into oviducts of surrogate females at day 1 of pseudopregnancy. For strict comparison, eight mutant and control 2-cell embryos (Supplementary Table 4) were transferred into the left and right oviducts of recipients, respectively. Recipient mothers were euthanized at 8.5, 11.5 and 14.5 days of gestation and embryos were dissected. For embryos developed to term, caesarean section was performed on day 19 and living pups were nursed by lactating ICR females.

Isolation of male pronuclei. Male pronuclei, which were distinguished from female pronuclei on the basis of their size and distance from polar bodies were harvested from zygotes of PN3–4 stages by breaking the zona using Piezo drive (Prime Tech) and aspirating using a micromanipulator. At least 40 male pronuclei from control or Tet3-deficient zygotes were collected and subjected to bisulphite sequencing analysis.

Bisulphite sequencing. For DNA methylation analysis in oocytes, pronuclei from zygotes and pseudo-pronuclei from NT embryos with limited numbers, bisulphite conversion was performed in agarose beads as described³⁵. Unbiased amplification for methylated and unmethylated sequences was ensured by testing bisulphite PCR primers using a 1:1 mixture of unmethylated and *in vitro* methylated DNA fragments. The PCR products were cloned into pMD19-T vectors (Takara Inc.) and individual clones were sequenced by BGI Ltd, Shanghai. Bisulphite primer

information is presented in Supplementary Table 6. For the determination of the methylation state of each sequence, the experiment was performed at least twice starting from the isolation of cells, pronuclei and embryos.

DNA immunoprecipitation with anti-5mC and anti-5hmC antibodies. To detect the existence of 5hmC at *Line1* repeats in the paternal genome in mouse zygotes, >100 male pronuclei were harvested from zygotes at PN3-4 stages, digested with proteinase K and RNase A, and the genomic DNA was purified by phenol-chloroform extraction. The genomic DNA was mixed with 250 ng of carrier lambda DNA (*dam*⁻, *dcm*⁻) and fragmented by AluI digestion, heat-denatured (10 min, 95 °C), and immunoprecipitated as described previously³⁶ using 1 µg of anti-5hmC or anti-5mC antibodies (Eurogentec, BI-MECY-1000) and 10 µl Dynabeads (coupled with M-280 sheep anti-rabbit IgG for the 5hmC antibody or anti-mouse IgG for the 5mC antibody). qPCR was performed on a BioRad CFX96 Real-Time PCR Detection System for the input and immunoprecipitated DNA. Mouse genomic DNA (10 ng) from Dnmt TKO embryonic stem cells lacking DNA methylation³⁷ and thus containing no 5hmC, was used as negative control. Mouse sperm DNA was used for comparisons.

Nuclear transfer with intact and enucleated oocytes. NT was performed as described³⁸ with modifications¹⁹. Briefly, metaphase II-arrested oocytes were collected from superovulated B6D2F1 or CKO females, and cumulus cells were removed using hyaluronidase. In the standard NT procedure, the oocytes were collected from wild-type and Tet3 CKO females, and enucleated in a droplet of HEPES-CZB medium containing 5 µg ml⁻¹ CB using a blunt Piezo-driven pipette. After enucleation, the spindle-free oocytes were washed extensively and maintained in CZB medium up to 2 h before nucleus injection. The cumulus cells collected from superovulated *Oct4-EGFP* transgenic mice were aspirated in and out of the injection pipette to remove the cytoplasmic material and then injected into enucleated oocytes. The reconstructed oocytes were cultured in CZB medium for 1 h and then activated for 5–6 h in activation medium. For NT with intact oocytes, oocytes were activated for 20 min and then directly injected with cumulus cells. The reconstructed oocytes were activated for 5–6 h in activation medium.

Following activation, the reconstructed embryos were cultured in KSOM medium with amino acids at 37 °C under 5% CO₂ in air. Embryo imaging and EGFP quantification followed the same procedure as in the ICSI experiment described above. The EGFP levels were determined from *n* > 6 embryos at each stage.

27. Ge, Y. Z. *et al.* Chromatin targeting of de novo DNA methyltransferases by the PWWP domain. *J. Biol. Chem.* **279**, 25447–25454 (2004).
28. Liu, P., Jenkins, N. A. & Copeland, N. G. A highly efficient recombining-based method for generating conditional knockout mutations. *Genome Res.* **13**, 476–484 (2003).
29. Rodriguez, C. I. *et al.* High-efficiency deleter mice show that FLPe is an alternative to Cre-*loxP*. *Nature Genet.* **25**, 139–140 (2000).
30. Lomeli, H., Ramos-Mejia, V., Gertsenstein, M., Lobe, C. G. & Nagy, A. Targeted insertion of Cre recombinase into the TNAP gene: excision in primordial germ cells. *Genesis* **26**, 116–117 (2000).
31. Lewandoski, M., Wassarman, K. M. & Martin, G. R. *Zp3-cre*, a transgenic mouse line for the activation or inactivation of *loxP*-flanked target genes specifically in the female germ line. *Curr. Biol.* **7**, 148–151 (1997).
32. Szabó, P. E., Hubner, K., Scholer, H. & Mann, J. R. Allele-specific expression of imprinted genes in mouse migratory primordial germ cells. *Mech. Dev.* **115**, 157–160 (2002).
33. Kimura, Y. & Yanagimachi, R. Intracytoplasmic sperm injection in the mouse. *Biol. Reprod.* **52**, 709–720 (1995).
34. Abràmoff, M. D., Magalhães, P. J. & Ram, S. J. Image processing with ImageJ. *Biophotonics Int.* **11**, 36–42 (2004).
35. Hajkova, P. *et al.* DNA-methylation analysis by the bisulfite-assisted genomic sequencing method. *Methods Mol. Biol.* **200**, 143–154 (2002).
36. Weber, M. *et al.* Chromosome-wide and promoter-specific analyses identify sites of differential DNA methylation in normal and transformed human cells. *Nature Genet.* **37**, 853–862 (2005).
37. Tsumura, A. *et al.* Maintenance of self-renewal ability of mouse embryonic stem cells in the absence of DNA methyltransferases Dnmt1, Dnmt3a and Dnmt3b. *Genes Cells* **11**, 805–814 (2006).
38. Wakayama, T., Perry, A. C., Zuccotti, M., Johnson, K. R. & Yanagimachi, R. Full-term development of mice from enucleated oocytes injected with cumulus cell nuclei. *Nature* **394**, 369–374 (1998).